JACS
JOURNAL OF THE AMERICAN CHEMICAL SOCIETY

ARTICLE

pubs.acs.org/JACS

Mechanistic Elucidation of Intramolecular Aminoalkene Hydroamination Catalyzed by a Tethered Bis(ureate) Complex: Evidence for Proton-Assisted C−N Bond Formation at Zirconium

David C. Leitch, Rachel H. Platel, and Laurel L. Schafer*

Department of Chemistry, University of British Columbia, 2036 Main Mall, Vancouver, British Columbia V6T 1Z1, Canada

Supporting Information

ABSTRACT: A broad mechanistic investigation regarding hydroamination reactions catalyzed by a tethered bis(ureate) zirconium species, [ureate(2−)]Zr(NMe$_2$)$_2$(HNMe$_2$), is described. The cyclization of both primary and secondary aminoalkene substrates gives similar kinetic profiles, with zero-order dependence on substrate concentration up to ∼60−75% conversion, followed by first-order dependence for the remainder of the reaction. The addition of 2-methylpiperidine changes the observed substrate dependence to first order throughout the reaction, but does not act as a competitive inhibitor. The reactions are first order in precatalyst up to loadings of ∼0.15 M, indicating that a well-defined, mononuclear catalytic species is operative. Several model complexes have been structurally characterized, including dimeric imido and amido species, and evaluated for catalytic performance. These results indicate that imido species need not be invoked as catalytically relevant intermediates, and that the mono(amido) complex [ureate(2−)]Zr(NMe$_2$)(Cl)(HNMe$_2$) is much less active than its bis(amido) counterpart. Structural evidence suggests that this is due to differences in coordination geometry between the mono- and bis(amido) complexes, and that an equatorial amido ligand is required for efficient catalytic turnover. On the basis of the determination of kinetic isotope effects and stoichiometric reactivity, the catalytic turnover-limiting step is proposed to be a concerted C−H, C−N bond-forming process with a highly ordered, unimolecular transition state ($\Delta S^{\ddagger} = -21 \pm 1$ eu). In addition to this key bond-forming step, the catalytic cycle involves an on-cycle pre-equilibrium between six- and seven-coordinate intermediates, leading to the observed switch from zero- to first-order kinetics.

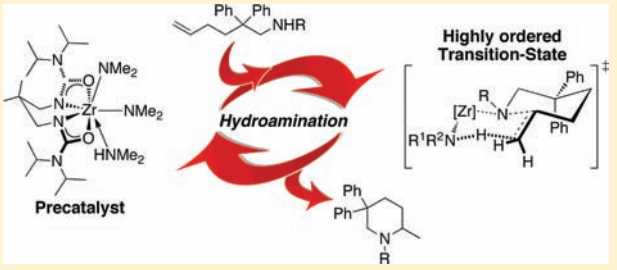

INTRODUCTION

Hydroamination reactions promoted by metal-based catalyst systems are proving to be an increasingly successful and widely applicable method for the synthesis of many important classes of nitrogen containing compounds.[1,2] Among the most promising catalysts in terms of synthetic applicability, economic viability, and low environmental impact are those incorporating group 4 metal ions. Since the first reports of group-4-mediated hydroamination in the early 1990s,[3−5] a plethora of research has been directed toward the discovery of efficient titanium and zirconium catalysts.[6−13] Elucidation of the mechanistic details of hydroamination reactions catalyzed by these systems is particularly important for further catalyst development and optimization.

In a landmark contribution, Bergman and co-workers described the mechanism of intermolecular alkyne hydroamination catalyzed by Cp$_2$Zr(NHR)$_2$ complexes (Scheme 1A).[3] The key step of this proposed pathway is a [2 + 2] cycloaddition between an imidozirconium intermediate and the alkyne substrate.[6] Subsequent turnover-limiting protonolysis of the Zr−C bond by an incoming amine substrate followed by an intramolecular proton-transfer releases the hydroamination product and regenerates the imidozirconium species. Subsequent mechanistic studies by Pohlki and Doye[14] and Johnson and Bergman[15] on the related titanium catalyst system Cp$_2$TiMe$_2$ strongly support this proposed cycloaddition pathway with alkyne and allene substrates.

As a result of substantial catalyst development efforts by many research groups, the catalytic intramolecular hydroamination of select aminoalkenes is now viable with a number of titanium and zirconium complexes.[16−47] Mechanistic work reported by Scott and co-workers,[28,44] and our own research group,[20] strongly supports a Bergman-type cycloaddition mechanism[3] for neutral catalysts with sterically encumbering ligand systems. One common mechanistic probe for the intermediacy of a catalytically active imido species is the demonstration that secondary aminoalkenes are not cyclized. While the vast majority of group 4 catalysts exhibit this substrate selectivity, a few reported examples do not obey this trend. These include cationic species that only cyclize secondary aminoalkenes[16,17] and rare neutral complexes that cyclize both primary and secondary substrates.[25,29,31,35,43] A kinetic analysis of catalytic reactions involving zirconium precatalysts supported by constrained-geometry ligands led Stubbert and Marks to propose a catalytic cycle wherein the key step involves an insertion of the alkene into a zirconium−amido bond (Scheme 1B),[25] similar to the mechanism determined for rare-earth catalysts.[48]

Received: March 30, 2011
Published: August 18, 2011

Scheme 1. (A) Simplified Cycloaddition Mechanism Proposed for Zirconocene Catalysts;[3] (B) Simplified Insertion Mechanism Proposed for CGC−Zr Catalysts;[25] and (C) Simplified Concerted C−N, C−H Bond Formation Mechanism Proposed for Oxazolinylborate−Zr Catalysts[55]

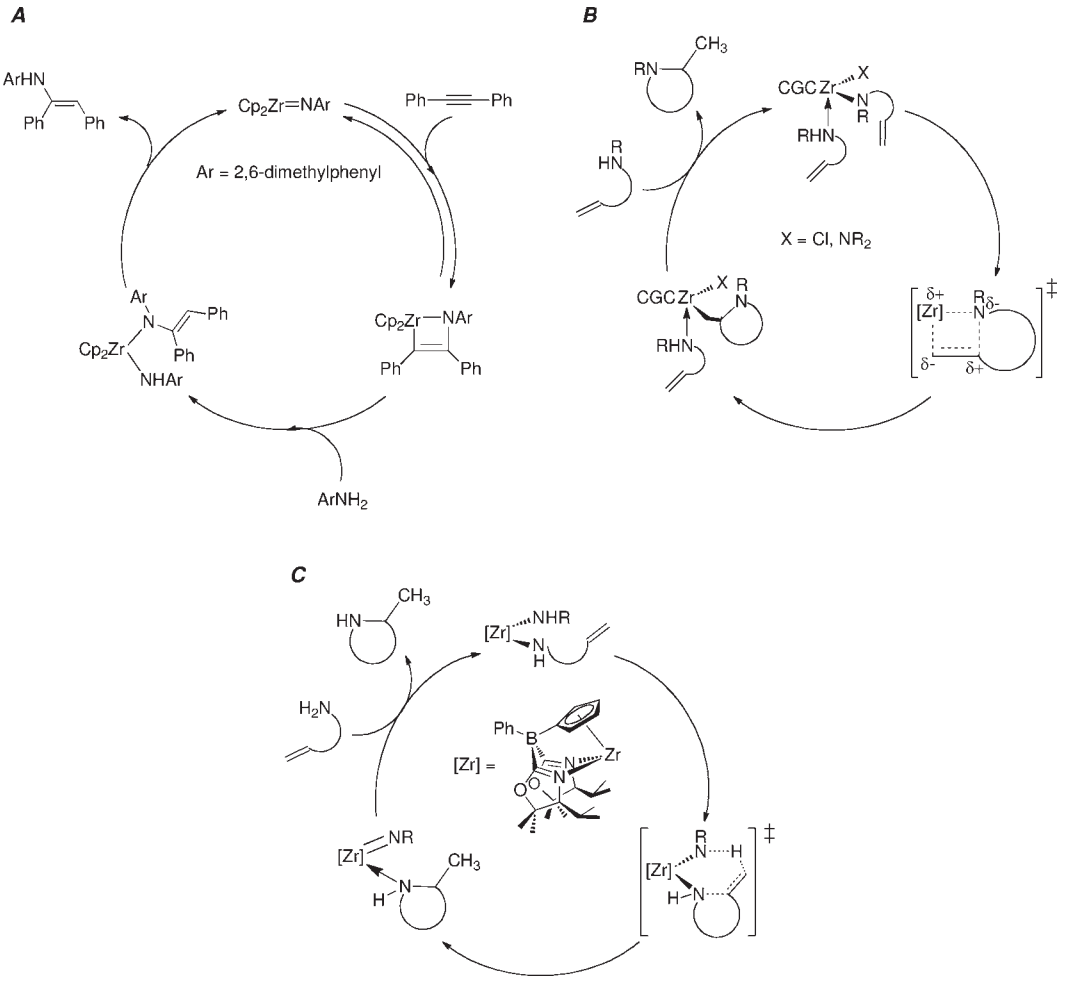

In a previous communication, we reported the development of a tethered bis(ureate) zirconium catalyst (**1**, Figure 1) for the intermolecular hydroamination of alkynes and the intramolecular hydroamination of alkenes.[35] This catalyst possesses unprecedented reactivity, generality, and functional group tolerance for a group 4 system. Precatalyst **1** performs effectively with both primary and secondary amines, forms 5-, 6-, and 7-membered rings via intramolecular hydroamination, operates in the presence of Lewis basic functional groups, and is chemoselective for the hydroamination product over a potentially competing α-alkylation reaction.[49−53] Thus, this system represents a unique example of a broadly applicable group 4 catalyst for alkene hydroamination, stemming directly from its ability to transform substrates that are inert to many, if not all reported group 4 systems. Understanding the source of this unique reactivity is therefore vital to further hydroamination catalyst development.

In an effort to elucidate the mechanistic pathway by which **1** promotes hydroamination, we have undertaken a broad mechanistic investigation involving both a kinetic analysis of catalytic reactions and an exploration of the stoichiometric chemistry of the precatalyst. We have determined that neither the imido-based cycloaddition mechanism nor the σ-bond insertion mechanism

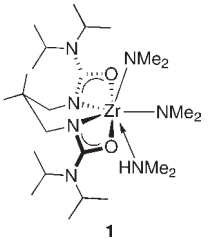

1

Figure 1. Tethered bis(ureate) precatalyst for hydroamination reactions.

(Scheme 1A and B) are accurate descriptions of the catalytic process. Instead, the evidence presented here points to a concerted C−H, C−N bond-forming event as the turnover-limiting step, as has been suggested within the field previously.[48,54] Importantly, a similar mechanistic model has been recently reported by Sadow and co-workers for an oxazolinylborate-supported zirconium catalyst.[55] Their model involves proton-transfer from a protic amido ligand to the alkene substrate in a six-membered transition state (Scheme 1C). This previous work provides important precedent for proton-assisted cyclohydroamination. In contrast to this system, for which a zirconium−imido complex is a key

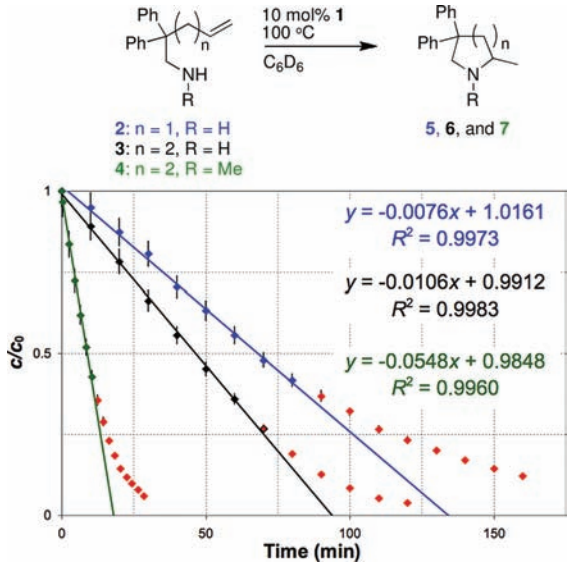

Figure 2. Plot of the consumption of aminoalkene substrates **2**−**4** (c/c_0) versus time (min) through approximately four half-lives. Red data points indicate exponential decay regime (not included in linear regression analysis). Error bars indicate ±5%.

intermediate, imido species do not appear to be catalytically relevant in reactions involving precatalyst **1**. This is an important distinction that explains the ability of **1** to efficiently cyclize both primary and secondary aminoalkenes.

RESULTS AND DISCUSSION

Empirical Rate Laws. To determine an empirical rate law for hydroamination reactions promoted by **1**, a kinetic analysis of aminoalkene cyclization has been undertaken. Figure 2 shows the results of monitoring the conversion of typical aminoalkene substrates (**2**−**4**) by ^{1}H NMR spectroscopy relative to an internal standard (1,3,5-trimethoxybenzene) in deuterated benzene. All of the reactions described herein have a high initial substrate concentration of 0.750 M, in accord with the conditions described previously for synthetic reactions.[35] ^{1}H NMR signals attributed to the protons of the ureate ancillary ligand can be observed in the spectra obtained during kinetic monitoring; unfortunately, these data are ambiguous as to the nature of the catalyst resting state.

The plots in Figure 2 clearly show a linear decay of substrate during the initial stage of the reaction (up to 65−75% conversion, best-fit line), indicative of zero-order dependence on aminoalkene concentration. Notably, cyclization to form 6-membered products **6** and **7** proceeds faster than that for the conversion of **2** to **5**. Finally, the conversion of the *N*-methylated secondary aminoalkene **4** occurs at a 5-fold higher rate than the cyclization of the analogous primary aminoalkene. This kind of catalytic behavior appears to be in contrast to other neutral d^0-metal-based catalysts, which have been reported to show higher activity for primary aminoalkenes over secondary substrates.[29,43,54,56−61]

Following the consumption of **2**−**4** reveals that at higher substrate conversion the plot becomes nonlinear (red points), exhibiting exponential decay consistent with first-order consumption of substrate. Furthermore, the onset of the nonlinear regime is dependent on the identity of the substrate: the rate of consumption of substrates **2** and **4** changes after ∼65% conversion, while that of **3** does not vary until ∼75% conversion. Kinetic profiles of this type often result from competitive inhibition by reaction products during the later stages of the reaction. Such product inhibition kinetics have been observed previously with rare-earth,[62−66] actinide,[25,57] and group 4[25] hydroamination precatalysts.

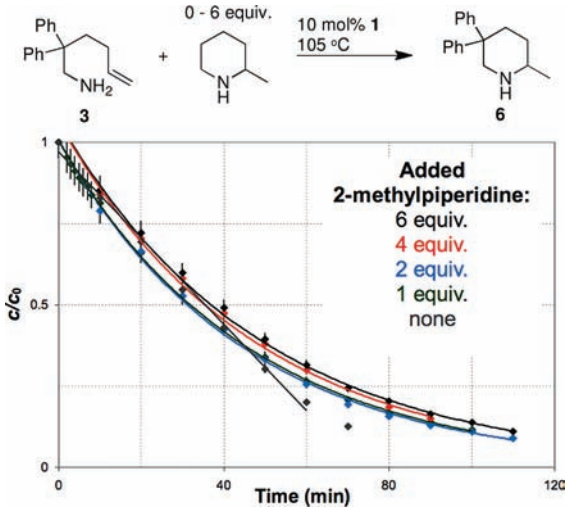

Figure 3. Plot of the consumption of **3** (c/c_0, $[\mathbf{3}]_0 = 0.75$ M) versus time (min) with added 2-methylpiperidine (0−6 equiv, up to 4.50 M); error bars indicate ±5%.

Table 1. Effect of Added 2-Methylpiperidine on the Conversion of 3

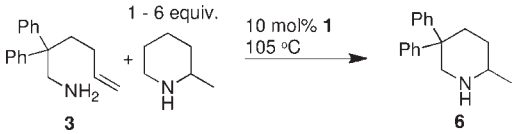

entry	[2-methylpiperidine] (M)[a]	k_{obs} (10^{-2} M min^{-1})[a,b]
1	0.750	2.19 ± 0.02
2	1.50	2.25 ± 0.04
3	3.00	2.13 ± 0.04
4	4.50	2.05 ± 0.03

[a] First-order rate constants. [b] Errors estimated from regression analysis of individual data points (single runs).

To investigate the possibility of competitive product inhibition during hydroamination catalysis, a series of reactions have been carried out with varying amounts of added 2-methylpiperidine. This specific inhibitor was chosen to mimic the structure of the hydroamination product **6**. Figure 3 illustrates the kinetic profiles of the conversion of **3** (105 °C) in the presence of 0−6 equiv (up to 4.50 M) of 2-methylpiperidine. Two striking features are observed for these reactions. First, there is no significant change in rate between the experiments with added inhibitor, despite the large excess of piperidine added to the latter reactions. Indeed, the difference in the pseudo-first-order k_{obs} across this 6-fold concentration range is less than 5% (Figure 3, Table 1). Thus, the reaction kinetics are largely unaffected by increasing the concentration of 2-methylpiperidine, meaning that this product-mimic is not a competitive inhibitor. More importantly, these results suggest that

dx.doi.org/10.1021/ja202448b |J. Am. Chem. Soc. 2011, 133, 15453–15463

Table 2. Aminoalkene Cyclization at Varying Precatalyst Concentrations

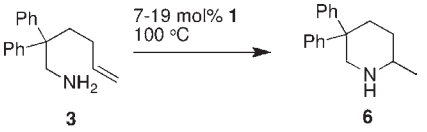

3 6

entry	[precatalyst] (M)[a] (mol %)	k_{obs} (10^{-3} min^{-1})[b]
1	0.0510 (6.8)	6.72 ± 0.12
2	0.0578 (7.7)	7.81 ± 0.15
3	0.0688 (9.2)	9.14 ± 0.10
4	0.0750 (10.0)	10.6 ± 0.2
5	0.104 (13.9)	16.4 ± 0.2
6	0.125 (16.7)	19.9 ± 0.4
7	0.127 (16.9)	20.0 ± 0.5
8	0.142 (18.9)	23.2 ± 0.4

[a] Precatalyst concentration determined at start of reaction by ^{1}H NMR spectroscopy through relative integration to internal standard, ±5%. [b] Errors estimated from regression analysis of individual data points (single runs).

competitive inhibition by product is not the source of late-reaction nonlinearity.

Second, the addition of 2-methylpiperidine does appear to change the reaction order in substrate throughout the entire course of the reaction. With no added piperidine, substrate consumption is linear until ~70% conversion (Figure 3, gray line). In contrast, substrate consumption is exponential if the piperidine is present. These data indicate that there is a change in the turnover-limiting step induced by the addition of 2-methylpiperidine. It is therefore likely that a similar change in mechanism, induced by high concentration of product (and concomitant low concentration of substrate), is responsible for the observed shift from zero- to first-order kinetics illustrated in Figure 2. Our rationale for this behavior will be discussed in terms of our overall mechanistic proposal in a subsequent section.

The above results indicate that there are two kinetic regimes for the conversion of aminoalkenes **2**−**4**, dependent upon the extent of reaction, and that the hydroamination product is not a competitive inhibitor of the reaction. To establish empirical rate laws for these two stages of the reaction, the rate of conversion of **3** was measured for a series of precatalyst concentrations (Table 2). A plot of the zero-order k_{obs} values obtained for the primary stage of the reaction versus [**1**] shows a linear correlation in the range [**1**] = 0.05−0.15 M (Figure 4).[67] Thus, there is a first-order dependence on catalyst concentration, giving the empirical rate law in eq 1 for the first stage of the hydroamination reaction. At high conversion, the empirical rate law in eq 2 is operative, with first-order dependence on both catalyst and substrate.

$$\text{primary stage : rate} = k[\text{catalyst}] \quad (1)$$

$$\text{secondary stage : rate} = k'[\text{substrate}][\text{catalyst}] \quad (2)$$

The Nature of the Active Catalyst. The first-order dependence on precatalyst concentration discussed in the previous section suggests that a well-defined, mononuclear catalytic species is present throughout the concentration range examined. Solid-state and

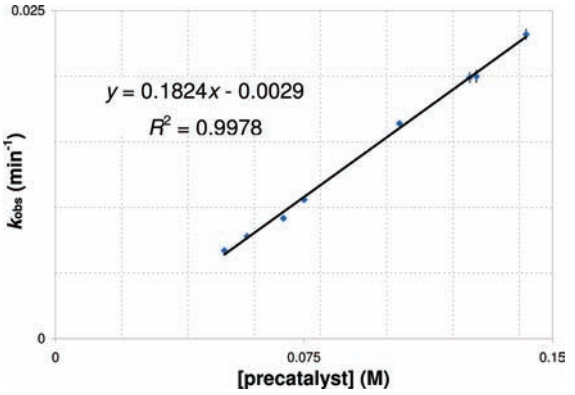

Figure 4. Plot of zero-order k_{obs} (min^{-1}) versus [precatalyst] (M), showing first-order dependence up to ~0.15 M. Error bars from estimated errors tabulated in Table 2.

solution-phase characterization of the precatalyst[35,68] also reveal mononuclear complexes. Notably, hydroamination reactions using Cp_2TiMe_2 as the precatalyst have a nonlinear catalyst dependence with [Cp_2TiMe_2] > 0.02 M, due to deactivation by reversible imido dimerization.[14] The fact that there is first-order behavior up to high concentrations of **1** (~0.15 M) is noteworthy, especially given the steric accessibility of the zirconium center in this case, as this accessibility may be anticipated to promote the formation of catalytically inactive dimers or higher aggregates. To ascertain why catalyst deactivation by dimerization is not kinetically relevant, model complexes derived from the precatalyst (**1**) have been prepared and studied. Given that both imido- and amido-based mechanisms are possible for the cyclization of primary aminoalkenes, studying the dynamic behavior of imido and amido species may help to determine if one or both are plausible catalytic intermediates.

Previously, we reported the synthesis of a bulky imido complex (**8**) supported by the same tethered bis(ureate) ligand through aminolysis of a dibenzyl complex.[69] X-ray crystallography indicates **8** is mononuclear in the solid state; however, this complex is observed to dimerize in solution to form a 1:1 mixture of **8** and **9** (eq 3). It therefore follows that imido species present during catalysis could be prone to this same dimerization. Notably, if the mixture of **8** and **9** is treated with excess pyridine (~10 equiv) and heated (65 °C), only complex **8** is observed. While pyridine is not present during catalytic reactions, this observation demonstrates that neutral ligands, such as the amine groups of aminoalkene hydroamination substrates or heterocyclic products formed, are capable of shifting the equilibrium in favor of the mononuclear species.

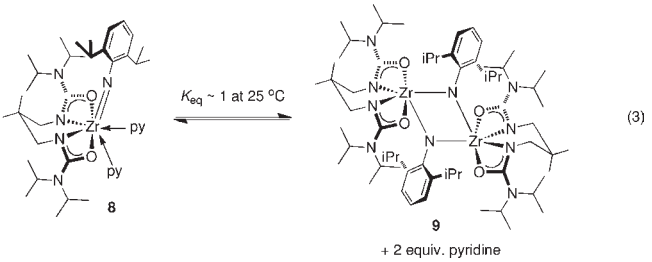

(3)

While the imido moiety of **8** is terminal, it is also very sterically demanding, especially in comparison to the aminoalkene substrates under investigation. To test if less bulky mononuclear imido complexes are accessible, 2,6-dimethylaniline has been

Scheme 2. Synthesis of Pyridine Adduct 10 and Dimeric Imido Complex 11

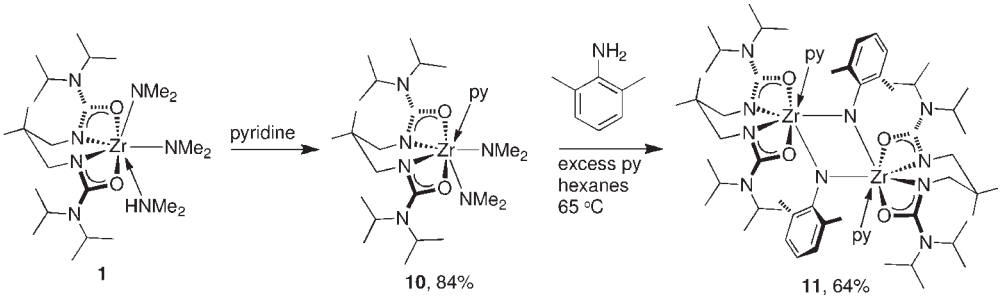

used to prepare an imido complex via the bis(amido) pyridine adduct **10**. A reaction between **10**, the aniline derivative, and excess pyridine at 65 °C yields a poorly soluble, pale yellow compound in 64% yield (Scheme 2). NMR spectroscopy reveals a ratio of ancillary ligand to 2,6-dimethylphenyl to pyridine of 1:1:1, consistent with an imido compound; however, the presence of only 1 equiv of pyridine suggests that the complex is a dimer (**11**), as the more sterically protected mononuclear imido complex **8** contains two stabilizing neutral ligands. Furthermore, there is only one observed component in solutions of **11**.

X-ray crystallography of **11** has confirmed the identity of the complex as dimeric in the solid state (Figure 5). Each half of the C_{2h}-symmetric molecule is related by an inversion center. The weakly bound pyridine ligands (Zr−N6: 2.557(1) Å) are in axial positions at the seven-coordinate zirconium centers. The ureate ligands deviate slightly from planarity, but to a much lesser degree than observed previously for the 2,6-diisopropylphenyl substituted dimer **9**.[69] In contrast to the monomer/dimer equilibrium observed between **8** and **9**, heating a mixture of **11** and excess pyridine to 65 °C does not result in any change to the spectral features. This indicates that, even in the presence of excess neutral ligands, **11** remains dimeric, or the monomer/dimer equilibrium heavily favors the dimer. Presumably, less bulky imido groups, such as those that would be formed with aminoalkene substrate, would favor dimerization to an even greater degree.

Notably, treatment of **8**, **9**, or **11** with a variety of alkynes and alkenes does not result in observable [2 + 2] cycloaddition reactions, the key step in imido-based hydroamination mechanisms (Scheme 1A).[3] The combination of facile dimerization observed in the formation of **11**, the fact that this dimer appears to persist in solution even in the presence of an excess of neutral ligand, the lack of evidence for dimerization or aggregation in reactions with precatalyst **1** (Table 2, Figure 4), and the unreactive nature of the Zr−N imido bonds in complexes **8**, **9**, and **11** toward stoichiometric cycloaddition lead us to rule out imido species as catalytically relevant intermediates for this system.

If imido species are not catalytically viable, then presumably the catalyst derived from **1** operates exclusively via amido-based intermediates that are structurally similar to precatalyst **1** and pyridine adduct **10**. Loss of the neutral ligand from either of these complexes would result in a coordinatively unsaturated species that could accommodate alkene coordination prior to insertion. Six-coordinate alkyl complexes supported by the same tethered bis(ureate) ligand have been isolated previously.[69] Synthesis of an analogous six-coordinate bis(amido) species has been attempted by subjecting solid **10** to high vacuum for 48 h (eq 4). Compound **10** was chosen for this purpose because the

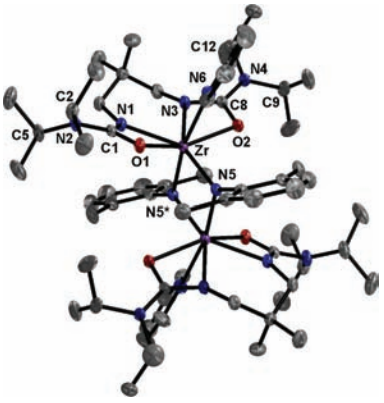

Figure 5. ORTEP representation of the molecular structure of **11** (ellipsoids plotted at 50% probability, hydrogens omitted) with selected bond lengths (Å), bond, and torsion angles (deg): Zr−N1, 2.2455(9); Zr−O1, 2.2373(8); Zr−N5, 2.1653(9); Zr−N5*, 2.0338(9); Zr−N6, 2.557(1); C1−N1, 1.321(1); C1−O1, 1.291(1); C1−N2, 1.361(1); N1−Zr−O1, 57.91(3); N1−Zr−N3, 74.21(4); N5−Zr−N6, 87.17(4); N5−Zr−N6*, 166.70(4); N5−Zr−N5*, 79.84(4); Zr−N6−Zr*, 100.16(4); N1−C1−N2−C5, 15.2(2); N3−C8−N4−C12, 42.6(2).

disappearance of pyridine can be easily monitored by NMR spectroscopy; however, similar treatment of **1** gives the same product **12**. The solid **10** changes from yellow to colorless during this period, and this new compound (**12**) has poor solubility in common organic solvents. The NMR spectra for product **12** are nearly identical to those of both **1** and **10**.

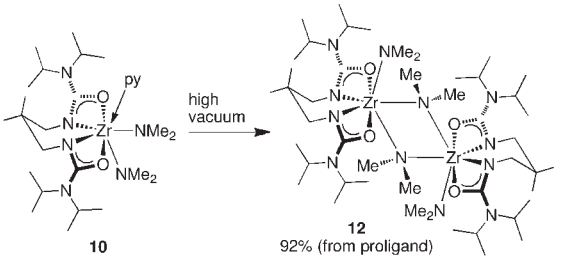

(4)

Compound **12** can be recrystallized from toluene for an X-ray crystallographic study (Figure 6), which confirms the structure as an amido-bridged dimer. This complex is structurally similar to the imido dimer **11**, exhibiting analogous C_{2h} symmetry. Each zirconium is seven-coordinate, as in the mononuclear parent complexes **1** and **10**. Two amido ligands are bound exclusively to one zirconium, with the remaining two bridging between the metal centers. This results in much longer Zr−N bonds for these

dx.doi.org/10.1021/ja202448b |J. Am. Chem. Soc. 2011, 133, 15453–15463

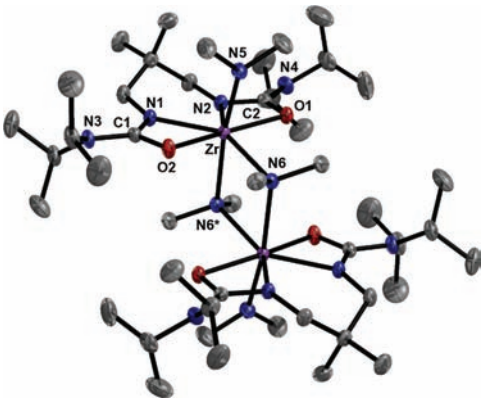

Figure 6. ORTEP representation of the molecular structure of **12** (ellipsoids plotted at 50% probability, hydrogens omitted) with selected bond lengths (Å), bond, and torsion angles (deg): Zr−N1, 2.241(1); Zr−O1, 2.226(1); Zr−N5, 2.108(1); Zr−N6, 2.323(1); Zr−N6*, 2.374(1); C1−N1, 1.312(2); C1−O2, 1.296(2); C1−N3, 1.373(2); N1−Zr−O2, 58.37(4); N1−Zr−N2, 74.43(4); N5−Zr−N6, 93.69(4); N5−Zr−N6*, 170.01(4); N6−Zr−N6*, 76.34(4); Zr−N6−Zr*, 103.66-(4); N1−C1−N3−C8, 44.1(2).

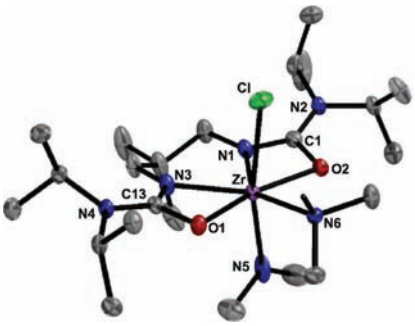

Figure 7. ORTEP representation of the molecular structure of **13** (ellipsoids plotted at 50% probability, hydrogens omitted) with selected bond lengths (Å), bond, and torsion angles (deg): Zr−N1, 2.195(2); Zr−O1, 2.180(2); Zr−N5, 2.171(2); Zr−N6, 2.397(2); Zr−Cl, 2.596(1); C1−N1, 1.353(3); C1−O1, 1.309(2); C1−N2, 1.322(3); N1−Zr−O1, 59.73(6); N1−Zr−N3, 78.33(6); Cl−Zr−N5, 167.10(5); sum of angles about N5, 359.6(6); sum of angles about N6, 341.0(4).

bridging amido groups (2.323(1) Å) relative to the terminal amido ligands (2.108(1) Å).

Attempts to observe a solution-phase equilibrium between **12** and a putative six-coordinate complex by variable-temperature NMR spectroscopy have been unsuccessful; however, the treatment of **12** with excess pyridine immediately regenerates **10** as judged by the distinct color change from colorless to yellow, and by the appearance of a broad pyridine signal at δ 8.61 ppm in the ^{1}H NMR spectrum, which is shifted slightly downfield from free pyridine (~8.5 ppm). These results suggest that in the presence of neutral donors, as is the case during catalysis, a neutral ligand stabilized seven-coordinate species is favored. Importantly, **12** can be used in catalytic hydroamination reactions with no decrease in reactivity relative to precatalyst **1**, verifying that catalyst deactivation via dimerization is not kinetically relevant. This is in excellent agreement with the previously discussed kinetic data that indicates first-order dependence on catalyst concentration (Table 2, Figure 4). The fact that **1** can operate at very high concentrations is important from a practical perspective as well, because reactions involving precatalyst **1** can be carried out efficiently with minimal solvent, reducing overall waste generation.

If the active catalyst derived from **1** does not access an imido intermediate, then presumably only one labile dimethylamido ligand is required in the precatalyst. Previously, Stubbert and Marks showed that a constrained-geometry-type zirconium hydroamination precatalyst with one dimethylamido ligand and one chloride ligand performs better than its bis(dimethylamido) analogue.[25] Notably, this catalyst has been postulated to mediate cyclohydroamination via a σ-bond insertion pathway (Scheme 1B). Modifying the structure of precatalyst **1** in the same manner would therefore provide an opportunity to test the viability of the insertion mechanism, and also to potentially improve catalytic activity. To investigate these questions, we have prepared an analogue to precatalyst **1** that contains one chloride ligand and one amido ligand (**13**). Complex **13** has been characterized by X-ray crystallography, with the solid-state molecular structure shown in Figure 7.

At first glance, the complex is closely analogous to the parent compound **1**, with the bis(ureate) ligand occupying the equatorial plane of a pentagonal bipyramid. However, there is one crucial difference: the anionic chloro and amido ligands are axial, and therefore trans to one another, whereas in precatalyst **1**, the two amido ligands are oriented cis, forcing one dimethylamido into an equatorial position. Previously reported results are consistent with the formal insertion of internal alkynes into the longer equatorial zirconium−amido bond;[68] we therefore anticipate that an intramolecular alkene insertion should also occur preferentially into an equatorial Zr−N_{amido} bond. Given that the sole amido ligand of **13** adopts an axial configuration, an amido ligand derived from an aminoalkene substrate will likewise have a thermodynamic preference for an axial coordination site, which may impact catalytic activity. Notably, the axial amido ligand in **13** has a remarkably long Zr−N5 distance of 2.171(2) Å, which is even longer than the equatorial Zr−N_{amido} bond of **1** (2.135(1) Å). Although the Zr−N5 length may suggest diminished multiple bond character, the geometry about N5 is planar, indicative of sp^2-hybridization and therefore some degree of Zr−amido π-bonding.

In contrast to the aforementioned zirconium constrained geometry systems,[25] use of **13** as a precatalyst for the hydroamination of aminoalkenes **2**, **3**, and **4** leads to a dramatic decrease in activity relative to the bis(amido) **1**. Only minimal conversion to product is observed under the reaction conditions, even for the secondary aminoalkene **4** (Scheme 3). Clearly, a weak Zr−amido bond is not a sufficient requirement for efficient hydroamination with this class of catalyst. In addition, all attempts to affect the stoichiometric insertion of internal alkynes into the axial Zr−N_{amido} bond of **13** using previously established reaction conditions[68] have been unsuccessful. These observations are consistent with the notion that an equatorial amido ligand is required for high catalytic activity with this class of catalyst.

The Nature of the Turnover-Limiting Step. The mechanistic evidence presented to this point definitively rules out an imido-based catalytic cycle and is consistent with an insertion-type catalytic cycle analogous to that proposed by Stubbert and Marks for the CGC−Zr systems (Scheme 1, B).[25] Kinetic data supporting this interpretation include the turnover-limiting intramolecular insertion of the alkene into a zirconium−amido bond, and the zero-order substrate dependence observed using **1** as a precatalyst. To further probe the nature of the turnover-limiting

Scheme 3. Low Activity of 13 When Used as a Hydroamination Precatalyst

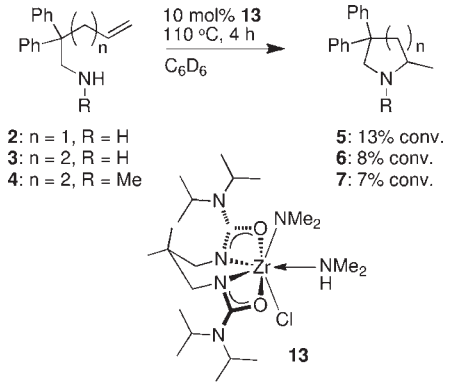

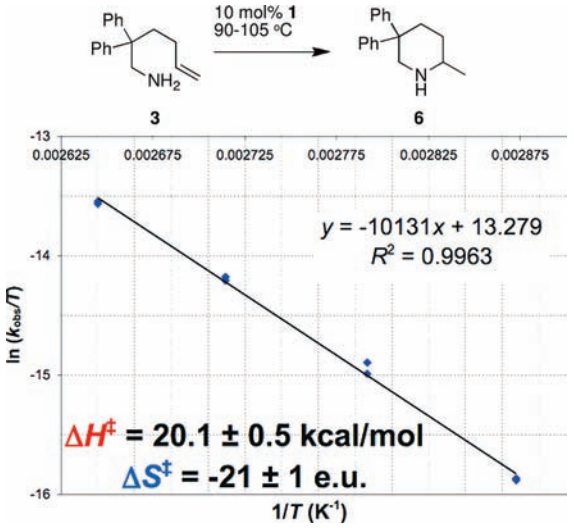

Figure 8. Eyring plot in the temperature range 75−105 °C for the cyclization of **3**; activation parameters as indicated; k_{obs} values represent zero-order rate constants determined over ~2 half-lives. Error on activation parameters represents standard error determined from regression analysis (see the Supporting Information for further details).

step, the temperature dependence of the cyclization rate of **3** has been investigated by determining the zero-order k_{obs} values at 10 °C intervals between 75 and 105 °C. The Eyring plot generated from these data is shown in Figure 8, along with the calculated activation parameters.

The $\Delta H^{\ddagger}$ value of 20.1 ± 0.5 kcal/mol and $\Delta S^{\ddagger}$ value of −21 ± 1 eu are similar to those determined for analogous cyclohydroamination reactions involving rare-earth catalysts,[48,62,63] actinide catalysts,[25] and CGC−Zr catalysts.[25] All of these systems are proposed to operate via σ-bond insertion, with the insertion step being turnover-limiting. The large and negative $\Delta S^{\ddagger}$ value suggests a highly ordered transition state, as would be expected from the proposed bicyclic transition state for alkene insertion (Scheme 1B). It should be noted that many mechanistic studies on imido-based catalytic cycles (Scheme 1A) have also yielded similar activation parameters, so a definitive statement regarding mechanism cannot be made solely from these data.

Notably, many lanthanide catalyst systems that are proposed to operate via σ-bond insertion exhibit large primary kinetic isotope effects (KIEs) when comparing *N*-proteo and *N*-deutero substrates,[48,65] meaning N−H bond cleavage is involved in the turnover-limiting step. These results would seem to contradict the notion of a simple intramolecular alkene insertion as being turnover-limiting. Previously, Marks and co-workers have proposed N−H bond involvement in the insertion transition state;[48] however, there have been no further investigations reported on this possibility with lanthanide catalysts. Recently, Sadow and co-workers have presented an alternate mechanistic interpretation, concerted C−H, C−N bond formation at magnesium- and zirconium-based systems (Scheme 1C), including the observation of primary KIEs for N−H/D substrates.[54,55]

To gauge the effect of *N*-deuteration on reactions with **1** as the precatalyst, the conversion of substrates d_2-**3** and *d*-**4** has been investigated. The cyclization of these aminoalkenes is much slower than for their proteo counterparts **3** and **4**, leading to k_H/k_D values of 5.2 ± 0.4 for **3**/d_2-**3** and 2.9 ± 0.2 for **4**/*d*-**4** (Figure 9). These primary KIEs are similar to the aforementioned values obtained with lanthanide catalysts (k_H/k_D = 2.7−5.2),[48,65] a magnesium catalyst (4.6),[54] and a zirconium catalyst (3.5).[55] This implies that a protonolysis event is turnover-limiting, either as a discrete step or as part of a concerted bond-forming process.

To investigate the possibility of stepwise insertion/protonolysis or concerted bond-formation, we endeavored to carry out model insertion reactions into zirconium−amido bonds supported by our tethered bis(ureate) ligand. As stated previously, we have observed the insertion of internal alkynes into the equatorial Zr−NMe_2 ligand of **1**.[68] To model analogous alkene insertion reactions, we have reacted **1** with an excess of a variety of activated alkenes, including styrene derivatives and norbornene. Unfortunately, after heating to 100−140 °C for several days, these reactions do not result in appreciable alkene consumption, and no discernible organometallic products have been observed. This is in accord with the inability of **1** to catalyze all attempted intermolecular alkene hydroamination reactions to date. Instead, our attention moved to investigate intramolecular insertion reactions, akin to those that would result in the cyclization of aminoalkene substrates during successful catalytic reactions.

Treatment of precatalyst **1** with either 1 or 2 equiv of the *N*-methylated aminoalkene **4** at 65 °C for 4 h does not give an insertion product, or even a substrate-derived bis(amido) complex. Rather, complete cyclization of **4** to **7** is observed, with no apparent change to the structure of the metal complex (Scheme 4, top). The dimethylamine liberated through aminolysis to form the initial zirconium−substrate complex presumably reacts with any Zr−C bond that may be formed via insertion to release the product **7**. In a similar fashion, treating **1** with 2 equiv of the *N*-methylated-aminopentene substrate **14** results in complete conversion to product **15** in 20 h without heating. Remarkably, this result reveals that **1** is capable of mediating intramolecular alkene hydroamination at room temperature. Only two other zirconium systems are able to perform this reaction under such mild conditions.[37,55]

To prevent the generation of a proton source that results in catalytic turnover to form the hydroamination products, the dialkyl complex **16** can be used as an alternate starting material. The absence of protic byproducts from aminolysis of **16** could possibly enable observation of putative organometallic insertion

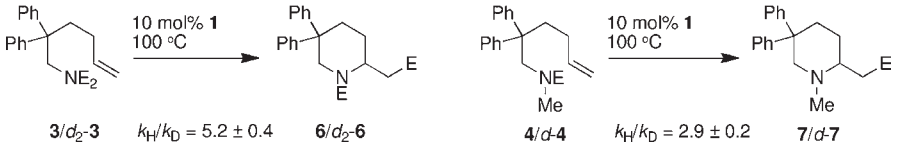

Figure 9. Primary kinetic isotope effects observed in the cyclization of aminoalkenes **3** and **4**.

Scheme 4. Attempted Observation of Intramolecular Insertion Reactions; Evidence for Proton-Assisted C−N Bond Formation

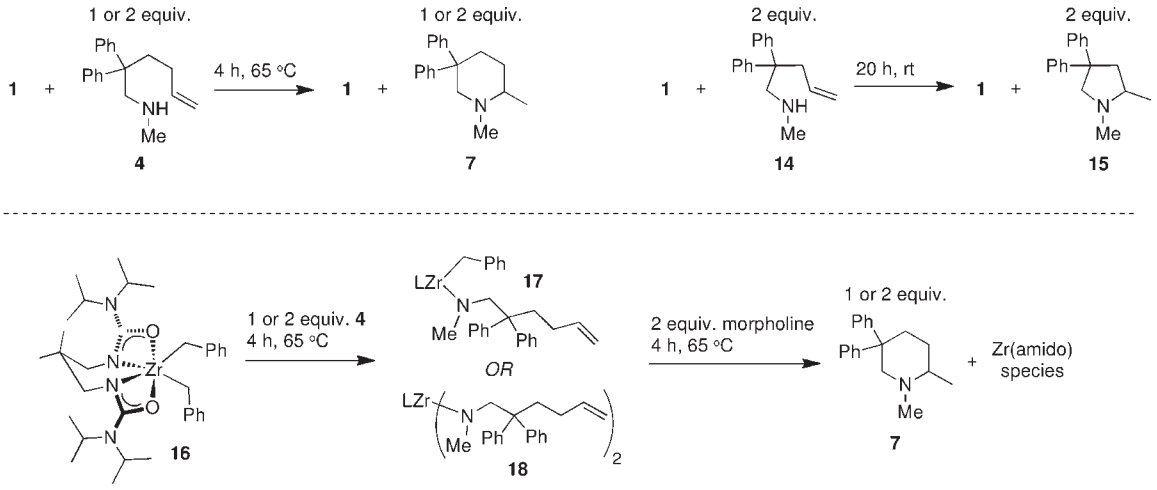

products; however, subjecting **16** to identical reaction conditions to those described above leads exclusively to the substrate-derived amido species (**17**,**18**) as judged by NMR spectroscopy, with the alkene moieties intact (Scheme 4, bottom). As C−N bond formation clearly occurs during stoichiometric reactions between **1** and **4**, the failure to observe insertion products from the reaction between **16** and **4** reveals that C−N bond formation in the absence of a proton source is not favored. As has been previously suggested,[48,54,55] a proton source may be required for C−N bond formation to occur. To further test this hypothesis, intermediates **17**,**18** have been treated with 2 equiv of morpholine. Upon heating to 65 °C for 4 h, complete conversion to product **4** is again observed. These experiments provide further evidence for proton-assisted C−N bond formation during catalytic reactions.[70]

Mechanistic Proposal. On the basis of the accumulated data regarding both thermodynamic and kinetic factors underlying the reactivity of **1** and related compounds, a plausible catalytic mechanism can be constructed. In a thermodynamic sense, it has been established that in the presence of neutral donors, zirconium dichloro,[71] dialkyl,[69] and bis(amido)[35] species supported by the tethered bis(ureate) ligand adopt a mononuclear, seven-coordinate, base-stabilized bonding motif. In contrast, zirconium imido fragments supported by this same ligand exhibit facile dimerization, even in the presence of excess donor, such as pyridine (Scheme 2, and eq 3); a mononuclear complex (**8**) can only be accessed by using a very large imido *N*-substituent and a significant excess of pyridine.[69] Furthermore, these imido compounds do not readily undergo [2 + 2] cycloaddition with alkynes to give metallacyclic products. These facts suggest that an imido-based, [2 + 2] cycloaddition mechanism[3] for hydroamination involving **1** is unlikely.

In contrast, σ-bond insertion of alkynes into the equatorial amido ligand of **1** has been observed previously, and concomitant formation of enamine side-products shows that hydroamination results from these reactions. Aminolysis of these metallacycles similarly forms enamines, thus establishing the feasibility of an insertion/protonolysis sequence for an alkyne hydroamination catalytic cycle with zirconium.[68] However, the results of attempted intramolecular insertions of alkenes into Zr−N bonds suggest that an amine proton source is required for C−N bond formation to occur with alkenes, in contrast to the previously observed alkyne insertion chemistry (Scheme 4).

Kinetically, the cyclization of aminoalkenes **2**−**4** has a zero-order dependence on substrate concentration, with a switch to first-order dependence occurring at high conversion (Figure 2), or with the addition of a product analogue (2-methylpiperidine, Figure 3). The cyclization of **3** is first order in catalyst up to [**1**] ≈ 0.15 M, revealing that the catalytically active species is well-defined, and not susceptible to deactivation at higher loadings. Given that both primary (**2** and **3**) and secondary (**4**) aminoalkenes exhibit similar kinetic profiles, it is reasonable that these substrates engage in the same mechanistic pathway, with the reduced reactivity observed for the primary amine substrate being attributed to some off-cycle imido complex formation. In addition, a primary KIE for the cyclization of *N*-deuterated substrates d_2-**3**, d-**4** indicates that N−H/D bond cleavage and/or C−H/D bond formation must be involved in the turnover-limiting step, consistent with a concerted C−H, C−N bond-forming process.[54,55] Finally, the $\Delta S^{\ddagger}$ for the cyclization of **3** is large and negative, providing evidence for a highly ordered transition state.

A proposed mechanism to account for all of these experimental observations is pictured in Scheme 5. This catalytic cycle is illustrated for the conversion of **3** to **6**; however, it should be equally accurate for the cyclization of other primary and secondary aminoalkenes. Initial aminolysis of the precatalyst by excess

Scheme 5. Proposed Catalytic Cycle for Intramolecular Alkene Hydroamination Using 1, with Derived Differential Rate Law (Steady-State Approximation for [A], [B], and [C])

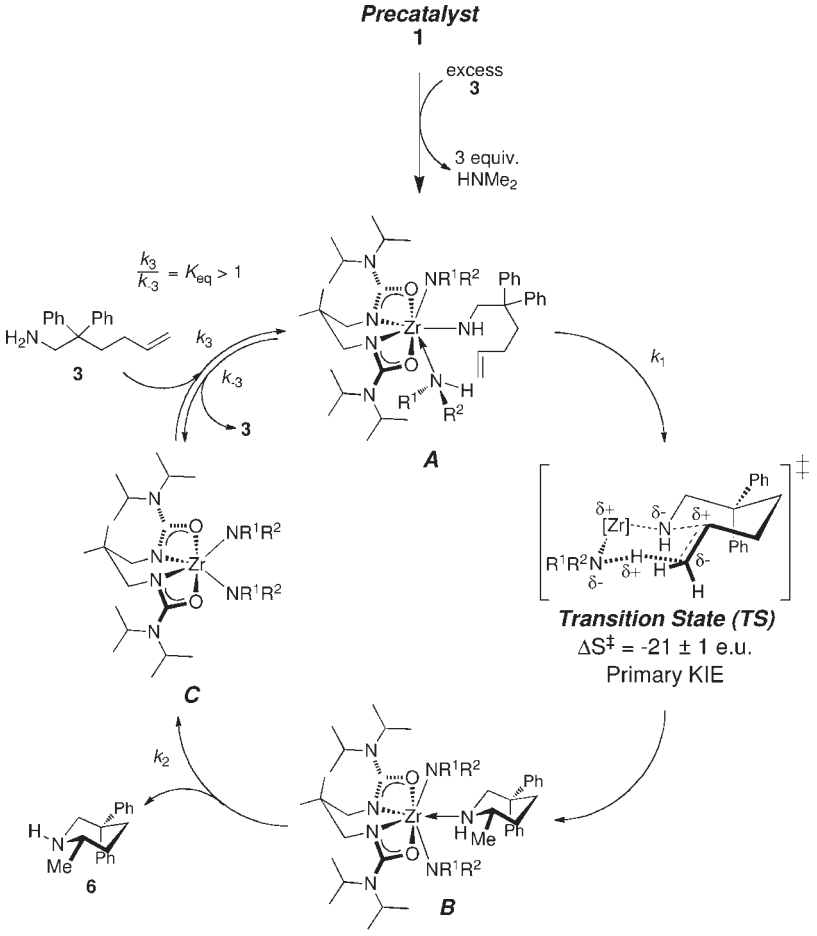

$$Rate = \frac{d[\mathbf{6}]}{dt} = \frac{k_1 k_2 k_3 [\mathbf{3}][\mathbf{1}]_0}{k_1 k_2 + k_1 k_3 + k_2 k_{-3} + k_2 k_3 [\mathbf{3}]}$$

substrate liberates dimethylamine to generate a structurally analogous bis(amido) species (**A**), which has a third substrate equivalent bound in an axial position. From this seven-coordinate state, intramolecular hydroamination takes place via irreversible C−H, C−N bond formation (k_1) through a highly ordered transition state (TS) involving a nucleophilic equatorial Zr−N bond and an acidic N−H from the axially bound amine ligand.

One interpretation of this concerted process is analogous to a transition state previously suggested by Marks and co-workers for rare-earth catalysts.[48] In this sense, a formal σ-bond insertion occurs via a four-membered transition state, involving the equatorial amido ligand and the alkene. Simultaneous protonation can also occur through a four-membered transition state between the N−H bond of the axial neutral amine ligand and the partial Zr−C bond. Alternatively, as suggested by Sadow and co-workers, this process can be viewed not as two connected four membered transition states, but as a single, chairlike six-membered transition state with no direct interaction between zirconium and the alkene (pictured in Scheme 1C).[54,55] A combination of both of these mechanistic extremes must also be considered. In either case, this concerted process would account for the large negative $\Delta S^{\ddagger}$, the primary KIEs, and the observed stoichiometric proton-assisted C−N bond formation represented in Scheme 4.[70]

Once cyclization has occurred at the equatorial Zr−N bond, the piperidine **6** would be neutrally bound in an equatorial position, forcing an electronically disfavored trans arrangement of two π-donating amido ligands (**B**). Rapid dissociation of **6** (k_2) would then generate a six-coordinate intermediate (**C**). This coordinatively unsaturated state can bind another equivalent of substrate (k_3) to regenerate a seven-coordinate species (**A**). This substrate binding is reversible (k_{-3}), leading to an equilibrium between catalytic intermediates **A** and **C**. On the basis of the observed preference for the binding of neutral donors, it can be deduced that this equilibrium favors the seven-coordinate species (i.e., $k_3 > k_{-3}$, or $K_{eq} > 1$). Applying the steady-state approximation for the concentrations of all catalytic intermediates, the differential rate law at the bottom of Scheme 5 can be derived. By making several reasonable assumptions regarding the relative magnitudes of the rate constants, this complex rate law can be simplified into two regimes that account for all of the kinetic behavior observed and are identical to the empirical rate laws derived from kinetic data (eqs 1 and 2).

dx.doi.org/10.1021/ja202448b |*J. Am. Chem. Soc.* 2011, 133, 15453–15463

In the first situation (primary stage of the reaction), neutral ligand association/dissociation is facile, and the rate constants k_2, k_3, and k_{-3} are likely much larger than k_1. In other words, the concerted bond formation (k_1) is the turnover-limiting step in the catalytic sequence. Because $k_1 \ll k_2$, k_3, and k_{-3}, all of the denominator terms containing k_1 can be neglected. Furthermore, as described in the previous paragraph, $k_3 > k_{-3}$, meaning $K_{eq} > 1$. Finally, during the initial stage of the reaction, the concentration of substrate is high; therefore, $k_2k_3[\mathbf{3}] \gg k_2k_{-3}$. Applying these assumptions gives the simplified rate law in eq 5, which is zero-order in [**3**] and first-order in $[\mathbf{1}]_0$. This is the same as the empirical rate law determined from kinetic experiments (eq 1). Furthermore, the only rate constant that contributes to the overall rate is k_1, which corresponds to the concerted bond-forming step. This same rate law can be derived in an intuitive fashion by assuming $k_1 \ll k_2$, k_3, and k_{-3}, and $[\mathbf{B}] + [\mathbf{C}] \ll [\mathbf{A}] \approx [\mathbf{1}]_0$. In this sense, catalytic turnover is dependent only on the concentration of the species **A**, which is much higher than that of **B** or **C**, and the rate constant of the bond formation (k_1).

The second stage of hydroamination catalysis, which exhibits first-order dependence on [**3**], occurs at high substrate conversion (eq 2), or with the addition of excess 2-methylpiperidine (Figure 3). To simplify the rate law from Scheme 5 to account for this kinetic behavior, the following assumptions can be made. First, k_1 is still much smaller than the other rate constants, so the denominator terms containing k_1 can be excluded in the same fashion as for eq 5. Second, at high conversion of **3**, the substrate concentration will be lower; therefore, $k_2k_{-3} \gg k_2k_3[\mathbf{3}]$. This has the effect of changing the turnover-limiting step to include both the equilibrium between **A** and **C** (K_{eq}) and the bond-forming step (k_1) (eq 6).

$$\text{Rate} = \frac{k_1k_2k_3[\mathbf{3}][\mathbf{1}]_0}{k_1k_2 + k_1k_3 + k_2k_{-3} + k_2k_3[\mathbf{3}]} = \frac{k_1k_2k_3[\mathbf{3}][\mathbf{1}]_0}{k_2k_3[\mathbf{3}]} = k_1[\mathbf{1}]_0 = k_{obs} \quad (5)$$

$$\text{Rate} = \frac{k_1k_2k_3[\mathbf{3}][\mathbf{1}]_0}{k_1k_2 + k_1k_3 + k_2k_{-3} + k_2k_3[\mathbf{3}]} = \frac{k_1k_2k_3[\mathbf{3}][\mathbf{1}]_0}{k_2k_{-3}} = k_1K_{eq}[\mathbf{3}][\mathbf{1}]_0 = k_{obs}'[\mathbf{3}] \quad (6)$$

Importantly, this second rate law accounts for both the observed first-order dependence on [**3**] and the observed zero-order dependence on added 2-methylpiperidine (Table 1, Figure 3). Because of the structural similarity between 2-methylpiperidine and the hydroamination product **6**, one can infer that the reaction should also be zero-order in [**6**]. If **6** were acting as a competitive inhibitor, the reaction should be inverse-order in product (or added 2-methylpiperidine). Notably, the addition of 2-methylpiperidine is observed to change the reaction to first-order in substrate throughout the course of the reaction, not just when the concentration of **3** is low. This suggests that 2-methylpiperidine, and by analogy the hydroamination product, is involved in the equilibrium between **A** and **C**. As the concentration of product increases, or if one or more equivalents of 2-methylpiperidine is added, the amido ligands on **A** and **C** will increasingly be derived from bulky piperidines (product/inhibitor) rather than acyclic amines (substrate). The presence of these bulky ligands would help to stabilize the six-coordinate species **C**, thus decreasing the equilibrium constant K_{eq}. If this decrease is large enough, then the term $k_2k_3[\mathbf{3}]$ would be much less than k_2k_{-3} (i.e., $k_2k_{-3} \gg k_2k_3[\mathbf{3}]$), leading to the same rate law given in eq 6. Work is currently underway to probe this proposed equilibrium between complexes similar to the intermediates **A** and **C** to assess this hypothesis.

CONCLUSIONS

Through a combination of elucidating stoichiometric reactivity patterns, and analyzing the kinetic profiles of catalytic reactions, a stereoelectronic proposal for the reactivity of zirconium precatalyst **1** has been presented. The ability of the catalytic species derived from **1** to efficiently cyclize both primary and secondary aminoalkenes stems directly from the steric and electronic environment imposed by the ancillary ligand. Use of this tethered bis(ureate) ligand provides steric accessibility to the metal center, enabling the favorable formation of seven-coordinate bis(amido) complexes that would facilitate a concerted C−H, C−N bond-forming event. Importantly, this renders precatalyst **1** more active for the cyclization of secondary aminoalkenes than primary substrates, behavior that is quite unique among neutral d^0-metal catalyst systems.[29,43,54,56−61]

The kinetic profile of aminoalkene cyclization indicates that the reaction proceeds through a unimolecular, highly ordered transition state. On the basis of the observation of proton-assisted C−N bond formation in stoichiometric reactions, and primary KIEs for cyclization of *N*-deuterated aminoalkenes, this transition state is proposed to involve concerted C−H and C−N bond formation. This can either be viewed as simultaneous σ-bond insertion of the alkene into the Zr−N bond and protonolysis of the partially formed Zr−C bond,[48] or as simultaneous nucleophilic attack by the amido ligand and protonation of the alkene.[54,55] These two interpretations differ in the role that zirconium plays in the process; in the former, the metal is directly involved in bond formation, while in the latter it is only indirectly involved. Furthermore, competitive product inhibition does not occur with this system, in contrast to many other d^0-metal catalyst systems.[25,57,62−66] Instead, two different kinetic regimes operate, depending on the relative concentrations of substrate and product. This dual reaction manifold is due to an on-cycle pre-equilibrium between a six-coordinate bis(amido) species and a seven-coordinate bis(amido)amine intermediate that can undergo concerted bond formation.

The insight regarding hydroamination catalysis gleaned as a result of this investigation sheds light on specific steric and electronic properties that can enable group 4 catalysts to perform hydroamination effectively with both primary and secondary amine substrates. With a mechanistic model in hand, ongoing work to prepare group 4 systems with further improved reactivity and selectivity patterns is targeted. The design of such systems, as well as further mechanistic and computational work exploring the proposed concerted bond formation pathway, is currently underway.

ASSOCIATED CONTENT

Supporting Information. Complete experimental details, kinetic plots, and CIFs for solid-state molecular structures. This material is available free of charge via the Internet at http://pubs.acs.org.

AUTHOR INFORMATION

Corresponding Author
schafer@chem.ubc.ca

ACKNOWLEDGMENT

We acknowledge funding from NSERC (CGSD to D.C.L., CRD Grant to L.L.S.), Imperial Oil Ltd., and Boehringer

Ingelheim (Canada) Ltd. in support of this work. R.H.P. thanks the Government of Canada (CBIE) for a Commonwealth postdoctoral fellowship.

REFERENCES

(1) Müller, T. E.; Beller, M. *Chem. Rev.* 1998, *98*, 675.
(2) Müller, T. E.; Hultzsch, K. C.; Yus, M.; Foubelo, F.; Tada, M. *Chem. Rev.* 2008, *108*, 3795.
(3) Walsh, P. J.; Baranger, A. M.; Bergman, R. G. *J. Am. Chem. Soc.* 1992, *114*, 1708.
(4) McGrane, P. L.; Jensen, M.; Livinghouse, T. *J. Am. Chem. Soc.* 1992, *114*, 5459.
(5) McGrane, P. L.; Livinghouse, T. *J. Am. Chem. Soc.* 1993, *115*, 11485.
(6) Duncan, A. P.; Bergman, R. G. *Chem. Rec.* 2002, *2*, 431.
(7) Bytschkov, I.; Doye, S. *Eur. J. Org. Chem.* 2003, 935.
(8) Doye, S. *Synlett* 2004, 1653.
(9) Odom, A. L. *Dalton Trans.* 2005, 225.
(10) Severin, R.; Doye, S. *Chem. Soc. Rev.* 2007, *36*, 1407.
(11) Lee, A. V.; Schafer, L. L. *Eur. J. Inorg. Chem.* 2007, 2243.
(12) Eisenberger, P.; Schafer, L. L. *Pure Appl. Chem.* 2010, *82*, 1503.
(13) Zi, G. *J. Organomet. Chem.* 2011, *696*, 68.
(14) Pohlki, F.; Doye, S. *Angew. Chem., Int. Ed.* 2001, *40*, 2305.
(15) Johnson, J. S.; Bergman, R. G. *J. Am. Chem. Soc.* 2001, *123*, 2923.
(16) Knight, P. D.; Munslow, I.; O'Shaughnessy, P. N.; Scott, P. *Chem. Commun.* 2004, 894.
(17) Gribkov, D. V.; Hultzsch, K. C. *Angew. Chem., Int. Ed.* 2004, *43*, 5542.
(18) Bexrud, J. A.; Beard, J. D.; Leitch, D. C.; Schafer, L. L. *Org. Lett.* 2005, *7*, 1959.
(19) Kim, H.; Lee, P. H.; Livinghouse, T. *Chem. Commun.* 2005, 5205.
(20) Thomson, R. K.; Bexrud, J. A.; Schafer, L. L. *Organometallics* 2006, *25*, 4069.
(21) Watson, D. A.; Chiu, M.; Bergman, R. G. *Organometallics* 2006, *25*, 4731.
(22) Lee, A. V.; Schafer, L. L. *Organometallics* 2006, *25*, 5249.
(23) Kim, H.; Kim, Y. K.; Shim, J. H.; Kim, M.; Han, M.; Livinghouse, T.; Lee, P. H. *Adv. Synth. Catal.* 2006, *348*, 2609.
(24) Wood, M. C.; Leitch, D. C.; Yeung, C. S.; Kozak, J. A.; Schafer, L. L. *Angew. Chem., Int. Ed.* 2007, *46*, 354.
(25) Stubbert, B. D.; Marks, T. J. *J. Am. Chem. Soc.* 2007, *129*, 6149.
(26) Marcsekova, K.; Loos, C.; Rominger, F.; Doye, S. *Synlett* 2007, 2564.
(27) Gott, A. L.; Clarke, A. J.; Clarkson, G. J.; Scott, P. *Organometallics* 2007, *26*, 1729.
(28) Gott, A. L.; Clarke, A. J.; Clarkson, G. J.; Scott, P. *Chem. Commun.* 2008, 1422.
(29) Majumder, S.; Odom, A. L. *Organometallics* 2008, *27*, 1174.
(30) Cho, J.; Hollis, K. T.; Helgert, T. R.; Valente, E. J. *Chem. Commun.* 2008, 5001.
(31) Müller, C.; Saak, W.; Doye, S. *Eur. J. Org. Chem.* 2008, 2731.
(32) Graebe, K.; Pohlki, F.; Doye, S. *Eur. J. Org. Chem.* 2008, 4815.
(33) Müller, C.; Koch, R.; Doye, S. *Chem.-Eur. J.* 2008, 10430.
(34) Zi, G.; Liu, X.; Xiang, L.; Song, H. *Organometallics* 2009, *28*, 1127.
(35) Leitch, D. C.; Payne, P. R.; Dunbar, C. R.; Schafer, L. L. *J. Am. Chem. Soc.* 2009, *131*, 18246.
(36) Reznichenko, A. L.; Hultzsch, K. C. *Organometallics* 2010, *29*, 24.
(37) Manna, K.; Ellern, A.; Sadow, A. D. *Chem. Commun.* 2010, *46*, 339.
(38) Bexrud, J. A.; Schafer, L. L. *Dalton Trans.* 2010, *39*, 361.
(39) Zi, G.; Zhang, F.; Xiang, L.; Chen, Y.; Fang, W.; Song, H. *Dalton Trans.* 2010, *39*, 4048.
(40) Zi, G.; Zhang, F.; Liu, X.; Ai, L.; Song, H. *J. Organomet. Chem.* 2010, *695*, 730.
(41) Xiang, L.; Zhang, F.; Zhang, J.; Song, H.; Zi, G. *Inorg. Chem. Commun.* 2010, *13*, 666.
(42) Wang, Q.; Song, H.; Zi, G. *J. Organomet. Chem.* 2010, *695*, 1583.
(43) Hu, Y.-C.; Liang, C.-F.; Tsai, J.-H.; Yap, G. P. A.; Chang, Y.-T.; Ong, T.-G. *Organometallics* 2010, *29*, 3357.
(44) Allan, L. E. N.; Clarkson, G. J.; Fox, D. J.; Gott, A. L.; Scott, P. *J. Am. Chem. Soc.* 2010, *132*, 15308.
(45) Janssen, T.; Severin, R.; Diekmann, M.; Friedemann, M.; Haase, D.; Saak, W.; Doye, S.; Beckhaus, R. *Organometallics* 2010, *29*, 1806.
(46) Antunes, M. A.; Munha, R. F.; Alves, L. G.; Schafer, L. L.; Martins, A. M. *J. Organomet. Chem.* 2011, *696*, 2.
(47) Ayinla, R. O.; Gibson, T.; Schafer, L. L. *J. Organomet. Chem.* 2011, *696*, 50.
(48) Gagné, M. R.; Stern, C. L.; Marks, T. J. *J. Am. Chem. Soc.* 1992, *114*, 275.
(49) Bexrud, J. A.; Eisenberger, P.; Leitch, D. C.; Payne, P. R.; Schafer, L. L. *J. Am. Chem. Soc.* 2009, *131*, 2116.
(50) Roesky, P. W. *Angew. Chem., Int. Ed.* 2009, *48*, 4892.
(51) Kubiak, R.; Prochnow, I.; Doye, S. *Angew. Chem., Int. Ed.* 2009, *48*, 1153.
(52) Prochnow, I.; Kubiak, R.; Frey, O. N.; Beckhaus, R.; Doye, S. *ChemCatChem* 2009, *1*, 162.
(53) Kubiak, R.; Prochnow, I.; Doye, S. *Angew. Chem., Int. Ed.* 2010, *49*, 2626.
(54) Dunne, J. F.; Fulton, D. B.; Ellern, A.; Sadow, A. D. *J. Am. Chem. Soc.* 2010, *132*, 17680.
(55) Manna, K.; Xu, S.; Sadow, A. D. *Angew. Chem., Int. Ed.* 2011, *50*, 1865.
(56) Hong, S.; Marks, T. J. *J. Am. Chem. Soc.* 2002, *124*, 7886.
(57) Stubbert, B. D.; Marks, T. J. *J. Am. Chem. Soc.* 2007, *129*, 4253.
(58) Yuen, H. F.; Marks, T. J. *Organometallics* 2008, *27*, 155.
(59) Yuen, H. F.; Marks, T. J. *Organometallics* 2009, *28*, 2423.
(60) Stanlake, L. J. E.; Schafer, L. L. *Organometallics* 2009, *28*, 3990.
(61) Broderick, E. M.; Gutzwiller, N. P.; Diaconescu, P. L. *Organometallics* 2010, *29*, 3242.
(62) Li, Y.; Marks, T. J. *J. Am. Chem. Soc.* 1996, *118*, 9295.
(63) Hong, S.; Kawaoka, A. M.; Marks, T. J. *J. Am. Chem. Soc.* 2003, *125*, 15878.
(64) Ryu, J. S.; Li, G. Y.; Marks, T. J. *J. Am. Chem. Soc.* 2003, *125*, 12584.
(65) Gribkov, D. V.; Hultzsch, K. C.; Hampel, F. *J. Am. Chem. Soc.* 2006, *128*, 3748.
(66) Giardello, M. A.; Conticello, V. P.; Brard, L.; Gagné, M. R.; Marks, T. J. *J. Am. Chem. Soc.* 1994, *116*, 10241.
(67) The plot of k_{obs} versus [precatalyst] has a nonzero intercept due to the moisture sensitivity of the catalyst and the impracticality of completely removing trace water from the aminoalkene substrate.
(68) Leitch, D. C.; Turner, C. S.; Schafer, L. L. *Angew. Chem., Int. Ed.* 2010, *49*, 6475.
(69) Leitch, D. C.; Schafer, L. L. *Organometallics* 2010, *29*, 5162.
(70) It should be noted that another possible pathway is consistent with the observed reactivity and kinetic profiles, fast reversible alkene insertion followed by slow intramolecular proton-transfer between a coordinated amine substrate and the Zr−C bond; however, this process would require a β-amide elimination reaction to occur as the reverse of alkene insertion. Observation of such a reaction has never been reported for group 4 or rare earth complexes. This pathway has previously been ruled out for lanthanide systems (see ref 48).
(71) Leitch, D. C.; Beard, J. D.; Thomson, R. K.; Wright, V. A.; Patrick, B. O.; Schafer, L. L. *Eur. J. Inorg. Chem.* 2009, 2691.